Laser-directed 3D assembly of carbon nanotubes using two-photon polymerization (Conference Presentation)

Conference Paper · April 2017

DOI: 10.1117/12.2257051

CITATIONS
2

READS
531

8 authors, including:

Ying Liu
University of Nebraska at Lincoln
20 PUBLICATIONS **386** CITATIONS
SEE PROFILE

Wei Xiong
100 PUBLICATIONS **1,677** CITATIONS
SEE PROFILE

L. J. Jiang
AdValue Photonics/Suzhou Tusen Laser
42 PUBLICATIONS **1,101** CITATIONS
SEE PROFILE

Yun Shen Zhou
University of Nebraska at Lincoln
164 PUBLICATIONS **2,814** CITATIONS
SEE PROFILE

Laser direct writing of multifunctional micro/nano devices using carbon nanotube–polymer composites

Paper No. 127

Y. Liu[1], W. Xiong[1, 2], L. J. Jiang[1], Y. S. Zhou[1], Lan Jiang[3], Jean-Francois Silvain[4] and Y. F. Lu[1]
[1]Dept. of Electrical and Computer Engineering, University of Nebraska-Lincoln, Lincoln, NE 68588-0511
[2]Wuhan National Laboratory for Optoelectronics, Huazhong University of Science and Technology, 1037 Luoyu Road, Wuhan, China, 430074
[3]School of Mechanical Engineering, Beijing Institute of Technology, Beijing 100081, China
[4]Institut de Chimie de la Matière Condensée de Bordeaux, Avenue du Docteur Albert Schweitzer Pessac F-33608 Cedex, France

Abstract

To unleash the full potential of two-photon polymerization (TPP) as a promising technique for three-dimensional (3D) fabrication of functional micro/nanostructures, multi-walled carbon nanotubes (MWNT) as filling materials were incorporated into polymer resins. Scanning electron microscopy images and polarized Raman spectra showed that the MWNTs with concentrations up to 0.2 wt % were uniformly distributed throughout the polymer matrix by thiol functionalization. A near-infrared femtosecond pulsed laser beam was focused into the composite resins, resulting in the 3D fabrication of arbitrary micro/nano architectures. The obtained MWNT-thiol-acrylate (MTA) composite structures exhibited significantly enhanced electrical conductivity and mechanical strength, and maintained high optical transmittance at the same time. Furthermore, MWNTs were self-aligned along the laser scanning direction in thiol-acrylate polymer, resulting in high electrical anisotropic effect of the MTA composites. Based on this highly conductive MTA composite photoresist, various functional micro/nano architectures and devices have been successfully fabricated, including photonic crystals, micromodels, microcapacitors and microresistors. Precise assembly of MWNTs with ~100 nm spatial resolution was achieved by the combination of TPP and direct pyrolysis. This technique enables 3D precise printing of multifunctional micro/nano devices and holds great potential to pave a way for wide applications of carbon nanotubes, such as 3D electronics, integrated photonics and micro/nanoelectromechanical systems (MEMS/NEMS).

Introduction

Carbon nanotubes (CNT) continue to deliver a huge impact on nanotechnology for their remarkable mechanical, electrical, thermal and optical properties. These properties make CNT potentially an ideal filling material for the preparation of polymer composites [1, 2]. Various approaches have been used for the fabrication of CNT-polymer composites, including solution processing of composites, melt spinning, melt processing, *in situ* polymerization, thermosets-based processing , electrospinning, and coagulation spinning for composite fibers and yarn production [3]. However, it is still challenging to achieve both high concentration and uniform dispersion of CNTs in the composites [4]. Moreover, the lack of precise controlled placement and alignment of CNTs in host polymer also limits the preparation and utilization of CNT based polymer composites.

Two-photon polymerization (TPP), also known as 3D direct laser writing (DLW) lithography, is a precision novel prototyping technology that offers the fabrication of complex volume structures with a superior nanometer resolution [5]. The multi-photon absorption is confined within the laser beam focal volume, allowing for the realization of arbitrary 3D printing. An ultrafine line width of ~ 40 nm and relatively high fabrication throughput with writing speed of 5 cm/s can be realized by TPP lithography [6]. The adaptability of the TPP technique is significantly determined by the properties of employed photoresist. Various functional materials, including carbon-based materials [7], photoisomerizable dyes [8], semiconductor nanoparticles [9] and metallic nanoparticles [10], were reported to be used in TPP lithography for fabrication of functional structures.

Adding CNTs to photoresist has been reported to be an effect way for CNT alignments in desired directions via TPP technique [7]. However, it is difficult to achieve both high CNT concentration and homogenous CNT dispersion due to the strong van der Waals interactions among individual CNTs. Moreover, the linear optical absorption of CNTs also limits the maximum CNT concentration in the composite resins

for the nonlinear TPP lithography [11]. The relatively low MWNT loading concentration leads to limited performance enhancement of the composite resins.

This paper reports a new TPP-compatible composite material based on multi-walled carbon nanotubes (MWNTs), thiol and acrylic photoresist. The obtained composite resins were demonstrated to have significantly enhanced electrical conductivity and mechanical strength, strong anisotropic properties and high optical transmittance. By the combination of TPP and direct pyrolysis, a precise control of MWNTs with ~100 nm spatial resolution was achieved. Based on the high electrical conductivity, microelectronic devices were fabricated, which could enable the applications of CNT in 3D electronics, integrated photonics, and micro/nanoelectromechanical systems (MEMS/NEMS).

Experimental

The TPP compatible host polymer was prepared by directly mixing acrylic monomer (di-trimethylolpropane tetraacrylate, Di-TMPTTA, Sartomer), thiol (pentaerythritol tetrakis (3-mercaptopropionate), PETMP, Sigma Aldrich) and photoinitiator (2-Benzyl-2-(dimethylamino)-4-morpholinobutyrophenone, BDMP, Sigma Aldrich). The branched structures of monomer PETMP and thiol Di-TMPTTA formed highly cross-linked networks. The photoinitiator BDMP was chosen for its high initiation efficiency and large absorbance in the 300 ~ 400 nm wavelength range [12]. Thiol and photoinitiator were used in all composite resins with constant concentration of 20 wt% and 1 wt%, respectively. Acid-purified MWNTs (Cheap Tubes Inc.) were directly added into the thiol-acrylate resins with various concentrations (0, 0.05, 0.1, 0.15 and 0.2 wt%). The mixtures underwent 90 s ultrasonic agitation (agitation power: 60 W, SONIFIER® SLPe Energy and Branson Ultrasonics) followed by magnetic stirring for 24 hours at room temperature (VWR, Standard hot plate stirrer) to achieve the uniform distribution of MWNTs. Ice bath was used during the ultrasonic process to avoid overheating of the composite resins. Before TPP fabrication, a purification process was applied using high-speed centrifuge (30 min @ 6000 rpm, mini spin 5452, Eppendorf) to remove large MWNT aggregations from the resins. The as-prepared resins showed excellent distribution of MWNTs with high concentrations and approved to be stable for one week without obvious MWNT aggregation under ambient conditions.

The TPP fabrications were carried out using a Photonic Professional GT system (Nanoscribe GmbH). Two-photon excitation is accomplished using 780 nm frequency-doubled output from an Er-fibre laser (1580nm, TEM_{00}, M^2<1.2) operating at 80 MHz with a temporal pulse duration ~100 fs. The printing of MTA resin via TPP lithography is shown in Fig 1. The fs laser was tightly focused into the MWNT-thiol-acrylate (MTA) resin to make 3D scans according to geometric user designs, resulting in solidified 3D micro/nanostructures with MWNTs simultaneously incorporated inside the polymer. After TPP lithography, the samples were developed for 20 mins in propylene glycol monomethyl ether acetate (PGMEA) followed by a soak in isopropyl alcohol (IPA). The unsolidified resin was rinsed away, leaving the 3D architectures of MTA composite polymer on the substrates.

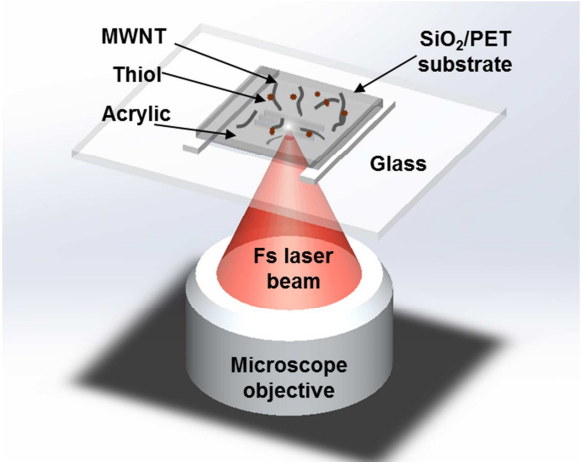

Fig.1 Schematic setup of 3D micro/nanofabrication of MTA composite resin by TPP lithography.

Characterization of the surface morphology was carried out by optical and scanning electron microscopy (SEM). SEM images were obtained using a Hitachi model S4700. To obtain high-quality images, the samples were sputter-coated with 5 nm of chromium. The imaging voltage was kept low (< 10 kV) to avoid damaging the structures. The polarized Raman microspectroscopy was conducted using a Raman microscope (Renishaw, InVia H 18415). The excitation laser beam, with a wavelength of 514.5 nm, was polarized after passing through a polarizer and focused onto a sample through an objective lens (50x, NA 0.75). The polarization direction was controlled using a half-wave plate placed between the objective lens and the polarizer. Raman scattering was collected using the same objective lens, and the polarization direction was rotated to be the same as that of the incident light. The average laser power and accumulation time used to produce Raman spectra was 10 mW and 10 sec, respectively. The Raman mapping was carried out with a grid spacing of 0.25 µm and an accumulation time of 3 seconds at each spot. The

optical absorption was measured using a UV-visible spectrophotometer (Evolution 201, Thermo Scientific). The mechanical properties were characterized by nanoindentation tests using a nanoindenter (TI 750 Ubi, Hysitron). A conical-shaped probe (TI-0093) with a tip radius of 3 μm was used. Working times were at 20 sec for the loading and unloading processes and 5 sec for holding at the maximum load to avoid creep behaviors. To characterize electrical conductivity, microwires were fabricated between two Au electrodes sputtering deposited on the desired regions through shadow masks (Kurt J. Lesker, 99.99% purity Au target). The *I-V* measurements of the microelectronic devices were conducted using a semiconductor parameter analyzer (Agilent HP4145C). The high frequency performances of the microresistors were measured by an impedance analyzer 4192A.

Results and Discussion

TPP fabrication of 3D micro/nanostructures

The TPP fabrication of micro/nanostructures based on MTA composite resin was independent of substrates, which can be conducted on either flexible polyethylene terephthalate (PET) or rigid substrates, including SiO_2/Si, silica, and glass. A broad range of functional micro/nanostructures was easily fabricated, including micro-coil inductor, woodpile, spiral-like photonic crystal, micro-engine inlet fan, micro-car model and micro-gear, as shown in Fig 2. The laser power and scanning speed used in the TPP fabrication were 15 mW and 0.5 mm/s, respectively.

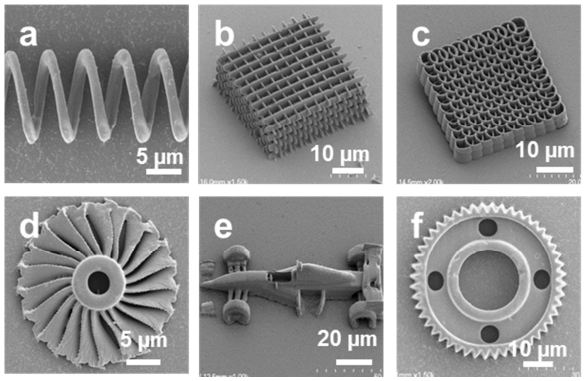

Fig. 2 SEM images of various functional micro/nanostructures fabricated using MTA composite resins by TPP lithography, including (a) micro-coil, (b) woodpile, (c) spiral-like photonic crystal, (d) micro-engine inlet fan, (e) micro-car model and (f) micro-gear.

Distribution and alignment of MWNTs

Characteristic G and D bands of the MWNT fingerprints were observed in the composite structures, as shown in Fig 3(a). The increasing G-band intensities matched with the increasing MWNT concentrations from 0 to 0.2 wt%. To analyse the spatial distribution of MWNTs, Raman mapping was conducted based on G band intensities of "TPP" logo fabricated using composite resin with 0.1 wt% MWNTs concentration. The Raman image matched the SEM image of the corresponding structures, indicating that the MWNTs were uniformly distributed throughout the whole structure, as shown in Fig 3(b). The uniform distribution of MWNTs in host polymer is ascribed to thiol functionalization. The thiol molecules are believed to be anchored onto the CNT surfaces [4], forming covalent functionalization of the MWNTs [13].

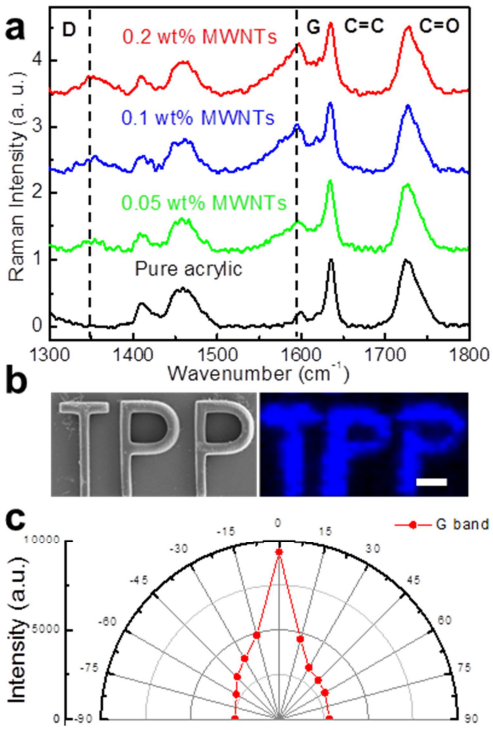

Fig. 3 (a) Normalized Raman spectra of microcubes fabricated using MTA composite resins with 0, 0.05, 0.1, and 0.2 wt% MWNT concentrations. A constant laser power of 6 mW and a writing speed of 100 μm/s were used for all cases. (b) Raman mapping image of the corresponding TPP pattern using the G-band of the MWNTs. The scale bar is 5 μm. (c) Polar-diagram of the G-band intensities as functions of the angle θ between the polarization of the excitation laser and the wire axis.

The alignment of MWNTs inside polymer matrix was characterized by polarized Raman spectroscopy of a

straight wire fabricated using composite resin with 0.1 wt% MWNTs concentration, as shown in Fig 3(c). The peak intensity of the G-band became strongest when the laser polarization was parallel with the axis of the wires (θ = 0°), then decreased to weakest when the laser polarization was perpendicular to the wires (θ = 90°). The reasons for the MWNT alignment inside the composite polymer are ascribed to the spatial confinement effect and volume shrinkage [7]. The length of MWNTs is longer than the laser focal volume, so the trapped MWNTs are forced to be aligned with the laser scan direction. Volume shrinkage can cause tensile strength along the wires, which also contributes to the alignment effect.

Precise assembly of MWNTs was achieved by the combination of TPP fabrication and direct pyrolysis based on the MTA composite resins. Due to the large difference of thermal stability between MWNTs and the acrylate polymer, the acrylate polymer was evaporated away and the MWNT bundles revealed, after thermal annealing at 500 °C in vacuum for 5 minutes. Fig 4 shows the linewidth of the single wire dropped from ~310 to ~100 nm with MWNT bundles remained on the substrate after polymer evaporation.

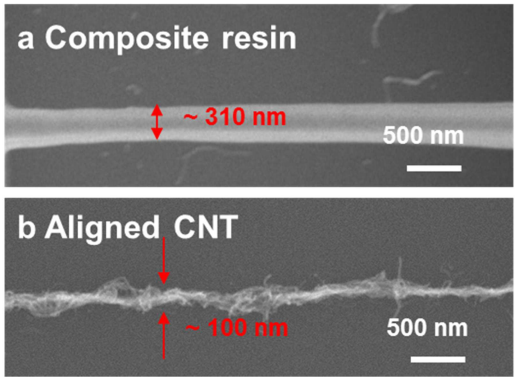

Fig. 4 SEM micrograph of a microline structure fabricated using MTA composite resin.

Properties enhancement of the MTA composite resin

Most photoresist is electronic insulating in pure or undoped states. By incorporating MWNTs into acrylic polymer, the composite resin changed from an insulator to a conductor. To investigate the electrical conductivity of the MTA composite polymers, microwires were fabricated between Au electrodes. Fig. 5(a) shows the conductivity of the MTA composite polymer increased drastically with increasing MWNT concentrations. With 0.2 wt% MWNTs loaded into the acrylate polymer, the electrical conductivity of the composite resin increased over 11 orders of magnitude and reached 46.8 S/m. The superior conductivity of the MTA composite polymers originated from the high MWNT concentration and the uniform MWNT distribution. Moreover, to verify the alignment effect of MWNTs in composites, two 5×5×75 μm^3 (W×H×L) bar-shaped channels between Au electrodes were fabricated with two orthogonal laser scanning directions, as shown in the inset of Fig 5(b). A three-orders-of-magnitude difference in electrical conductance was observed, which matched with the high anisotropy in electrical conductivity of CNTs in directions parallel with or perpendicular to the CNT axis.

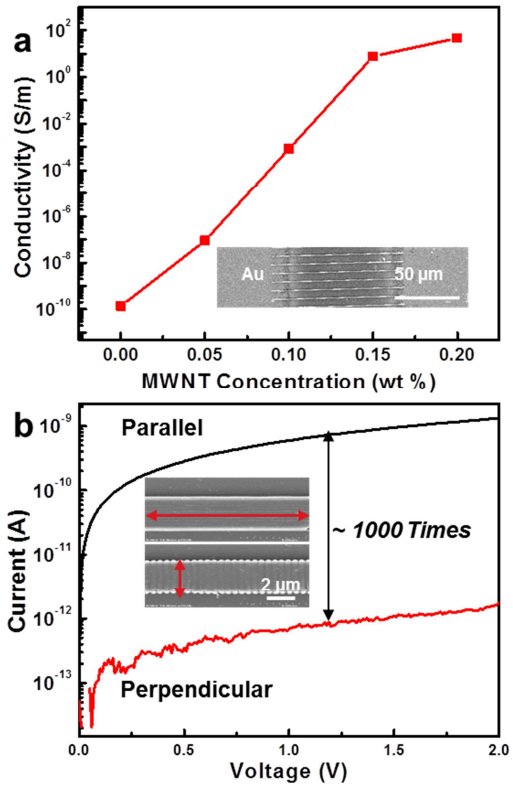

Fig. 5 (a) Electrical conductivity of the MTA composites with respect to the MWNT concentrations. The inset shows microwires fabricated between Au electrodes. (b) The *I-V* curve of two bar-shaped channels with two orthogonal laser scanning directions. The inset shows SEM images of channels and corresponding laser scanning directions.

Other than high electrical conductivity, the mechanical strength of the composite resin was also proved to be greatly enhanced by the reinforcement effect of MWNTs. Fig. 6(a) shows the loading and unloading curves of nanoindentation for microcubes. With 0.1 wt% MWNTs loading, the reduced Young's modulus increased from 1.35 ± 0.15 GPa to 1.90 ± 0.2 GPa, the

hardness increased from 43 ± 0.8 KPa to 67.5 ± 0.9 KPa. Two suspended microbridges with the same design were fabricated using acrylic resin (MWNT 0 wt%) and MTA composite resin (MWNT 0.1 wt%) by scanning a laser beam from one cubic support to another in a layer-by-layer manner. Under the same fabrication conditions (laser power: 30 mW, scanning speed: 10 mm/s), the bridge made by acrylic resin deformed seriously, while the one fabricated by the MTA composite resin remained straight without any obvious deformation, indicating the enhanced mechanical strength by MWNT loading. It was found that the loading of MWNTs can significantly enhance the mechanical performance of the microstructures fabricated by TPP lithography.

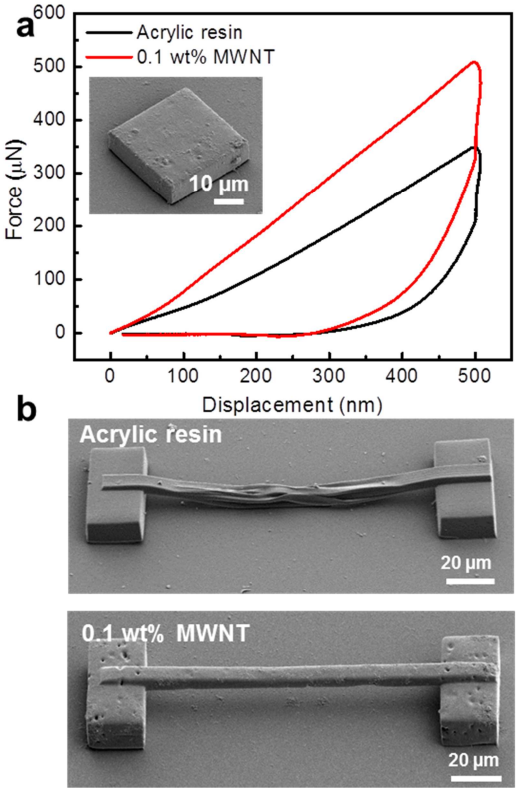

Fig. 6 (a) Loading and unloading curves of nanoindentation for microcubes fabricated using acrylic and MTA composite resin. The inset is the SEM image of a microcube fabricated using MTA composite resin. (b) The SEM images of microbridges fabricated using acrylic resin and MTA composite resin.

In addition, we examined the optical transmission properties of 6 μm MTA composite thin films cured by UV exposure. Fig. 7(a) shows the transmission spectra of the thin films with MWNT concentration increased from 0 to 0.2 wt%. The corresponding transmittance decreased slowly from 99 to 94% at 550 nm, as shown in Fig. 7(b). The inset image indicates the excellent optical transparency of the thin film on quartz substrate fabricated using MTA composite resin with 0.1 wt% MWNT concentration.

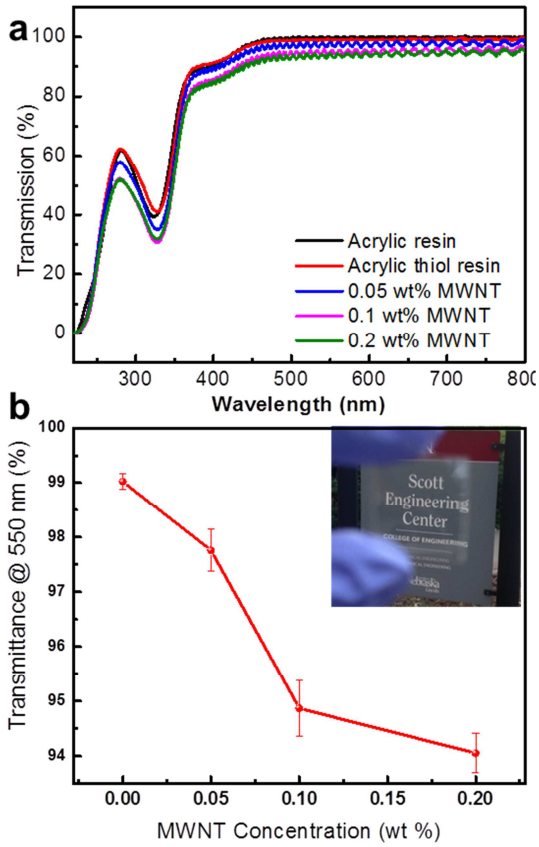

Fig. 7 (a) Optical transmittance spectra of the MTA composite thin films with respect to the MWNT concentrations. (b) Transmittance of the MTA composite thin films at a wavelength of 550 nm. The inset shows the optical image of a composite thin film fabricated using MTA composite resin with 0.1wt% MWNT concentration.

Application of multifunctional MTA composites

To demonstrate the potential of the MTA composite resins, we fabricated a series of microelectronic devices, including arrays of capacitors (Fig. 8(a)) and resistors (Fig. 8(c)) on SiO_2/Si substrates. The MWNT concentration of the composite resin was 0.1 wt%. Fig. 8(c) shows a typical hysteresis loop of a capacitor array containing 10 microcapacitors in parallel. The capacitance was measured to be 50 pF. Fig. 8(d) shows the frequency responses of a resistor array containing 20 zigzag microresistors in parallel and copper micro-ribbon fabricated by Cu sputtering through a shadow mask. With frequency lower than 100 KHz, relatively

stable impedances were obtained with both composite polymer (~ 90 KΩ) and copper (~ 900 Ω) lines. In high frequency range, the impedance of copper ribbon remained stable from 100 KHz to 10 MHz, and then increased slightly due to the increasing skin effect. However, the impedance of the MTA polymer transmission line decreased exponentially from 90,000 to 808 Ω from 100 KHz to 10 MHz, which is even lower than that of the Cu ribbon when the frequency was larger than 8 MHz. This phenomenon can be ascribed to the effective mitigation of the skin effect by the MWNTs [14]. Therefore, the MTA composite polymer is promising for potential application at high frequency range such as RF electronics.

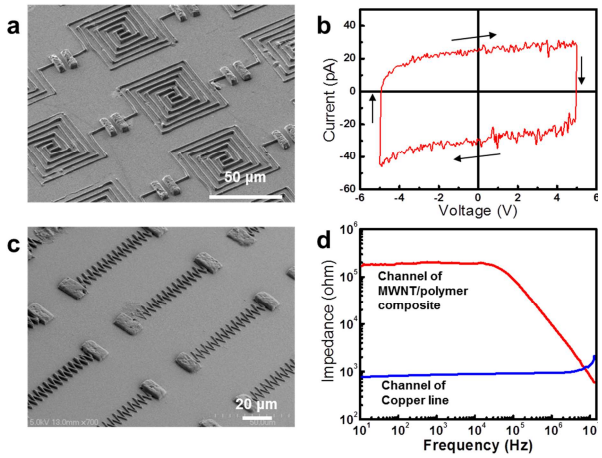

Fig 8 (a) The SEM image of a microcapacitors array. (b) Hysteresis loop of the 10 microcapacitors connected in parallel capacitors (scanning frequency at 0.025 Hz). (c) The SEM image of a micro-resistors array with zigzag shape. (d) Frequency responses of transmission lines made of MTA composite and copper as a reference. .

Conclusions

In summary, a TPP-compatible, homogenous MTA resin with high MWNT concentrations (up to 0.2 wt%) has been developed. Various functional 3D micro/nanostructures using the MTA resins have been successfully developed via TPP lithography. Precise MWNT assembly of ~100 nm spatial resolution has been achieved by the combination of TPP lithography and the subsequential thermal pyrolysis process. The MTA composite exhibits multifunctional reinforced properties, including increased mechanical strength, high optical transparency, enhanced electrical conductivity and flexible to both soft and rigid substrates. Based on the highly conductive MTA composite polymers, we have successfully fabricated various microelectronic devices, including capacitors and resistors. 3D printing of micro/nanostructures using highly conductive MTA composites paves the way toward arbitrary precise assembly of MWNTs, which is promising for a broad range of device applications such as 3D electronics and MEMS/NEMS.

Acknowledgements:

This research work was financially supported by the National Science Foundation (Grant No. CMMI 1265122) and Nebraska Center for Energy Sciences Research.

References:

1. Thostenson, E. T., Li, C., & Chou, T. W. (2005). Nanocomposites in context. Composites Science and Technology, 65(3), 491-516.
2. Fujigaya, T., Haraguchi, S., Fukumaru, T., Nakashima, N. (2008). Development of novel carbon nanotube/photopolymer nanocomposites with high conductivity and their application to nanoimprint photolithography. Advanced Materials, 20(11), 2151-2155.
3. Byrne, M. T., & Gun'ko, Y. K. (2010). Recent advances in research on carbon nanotube–polymer composites. Advanced Materials, 22(15), 1672-1688.
4. Gao, C., Jin, Y. Z., Kong, H., Whitby, R. L., Acquah, S. F., Chen, G. Y. & Fearon, P. (2005). Polyurea-functionalized multiwalled carbon nanotubes: synthesis, morphology, and Raman spectroscopy. The Journal of Physical Chemistry B, 109(24), 11925-11932.
5. Sun, H. B., & Kawata, S. (2004). Two-photon photopolymerization and 3D lithographic microfabrication. In NMR• 3D Analysis• Photopolymerization (pp. 169-273). Springer Berlin Heidelberg.
6. Bückmann, T., Thiel, M., Kadic, M., Schittny, R., & Wegener, M. (2014). An elasto-mechanical unfeelability cloak made of pentamode metamaterials. Nature communications, 5.
7. Ushiba, S., Shoji, S., Masui, K., Kono, J., & Kawata, S. (2014). Direct laser writing of 3D architectures of aligned carbon nanotubes. Advanced Materials, 26(32), 5653-5657.
8. Ishitobi, H., Shoji, S., Hiramatsu, T., Sun, H. B., Sekkat, Z., & Kawata, S. (2008). Two-

photon induced polymer nanomovement. Optics express, 16(18), 14106-14114.

9. Sun, Z. B., Dong, X. Z., Chen, W. Q., Nakanishi, S., Duan, X. M., & Kawata, S. (2008). Multicolor polymer nanocomposites: in situ synthesis and fabrication of 3D microstructures. Advanced materials, 20(5), 914-919.
10. Masui, K., Shoji, S., Asaba, K., Rodgers, T. C., Jin, F., Duan, X. M., & Kawata, S. (2011). Laser fabrication of Au nanorod aggregates microstructures assisted by two-photon polymerization. Optics express, 19(23), 22786-22796.
11. Guo, Q., Xiao, S., Aumann, A., Jaeger, M., Chakif, M. B., Ghadiri, R. & Ostendorf, A. (2012). Using Laser Microfabrication to Write Conductive Polymer/SWNTs Nanocomposites. Journal of Laser Micro/Nanoengineering, 7(1).
12. Nguyen, L. H., Straub, M., & Gu, M. (2005). Acrylate-Based Photopolymer for Two-Photon Microfabrication and Photonic Applications. Advanced Functional Materials, 15(2), 209-216.
13. Hirsch, A., & Vostrowsky, O. (2005). Functionalization of carbon nanotubes. In Functional molecular nanostructures (pp. 193-237). Springer Berlin Heidelberg.
14. D'Amore, M., Sarto, M. S., & D'Aloia, A. G. (2010). Skin-effect modeling of carbon nanotube bundles: the high-frequency effective impedance. In Electromagnetic Compatibility (EMC), 2010 IEEE International Symposium on (pp. 847-852). IEEE.